

CRYSTALLINE STATE DISORDER AND HYPERFINE COMPONENT LINE WIDTHS IN FERRIC HEMOGLOBIN CHAINS

DON A. HAMPTON AND ARTHUR S. BRILL, *The University of Virginia,
Department of Physics, Charlottesville, Virginia 22901 U.S.A.*

ABSTRACT In X-band electron paramagnetic resonance spectra from single crystals of horse ferric hemoglobin, observed line widths at the low- and high-field extrema are 30 and 24 G, and as much as 400 G in the intermediate region. This behavior is similar to that of ferric myoglobin. Due to large anisotropy in the g -tensors, the line width variation can be accounted for on the basis of heme orientation disorder. This disorder is characterized by an angle, determined here by two independent methods. In these computations Gaussian disorder on a sphere is assumed. The disorder angle is found to be constant on the sphere and about 4° for both α - and β - chains. Treatment of crystals with heavy water (buffer) increases the disorder. Since ligand nitrogen hyperfine couplings are available from hemoglobin electron nuclear double resonance, single crystal electron paramagnetic resonance spectra can be simulated by superimposing hyperfine bands, where the line width of the component bands is a variable and the disorder model above is employed. Comparison with observed resonances fixes the hyperfine component line widths. These component line widths from ferric hemoglobin in the crystalline state are found to be smaller than those in frozen solution.

INTRODUCTION

The line widths of the bands in electron paramagnetic resonance (EPR) spectra from transition metal ions in proteins are influenced by several aspects of structure, and hence contain structural information. For example, dipolar broadening arises from interactions with neighboring atoms, such as protons, nitrogens, and paramagnetic metal ions. However, factors other than these structural features of interest can be the major sources of broadening. One such factor in single crystal EPR is disorder of the magnetic centers. We describe below methods for characterizing this disorder and, with this knowledge, arriving at the line widths of component hyperfine bands in crystals. As an infinitely disordered system, frozen solution spectra can be similarly analyzed. The component line widths from ferric hemoglobin are found to be different in frozen solution than in the crystalline state.

METHODS

Horse red blood cells were obtained from Flow Laboratories, Inc. (Rockville, Md.). The hemoglobin was prepared according to the method of Brill et al. (1975) and further purified by passage through a carboxymethyl cellulose cation exchanger column (C-2758, Sigma Chemical Co., St. Louis, Mo.). Crystals were prepared by the method of Perutz (1968). All acid ferric hemoglobin concen-

Dr. Hampton's present address is: Alabama Power Company, Birmingham, Ala. 35291.

trations were determined spectrophotometrically with the absorptivities tabulated by Brill and Williams (1961). Deuterated crystals were prepared by successively soaking protonated crystals in deuterated mother liquor baths of increasing D₂O/H₂O content. (It was found that shattering occurred when protonated crystals were initially soaked in >95% deuterated mother liquor.) The total soak time was usually less than 12 h. For frozen solution samples, the heme concentration was 0.5 mM in 33 mM phosphate buffer at pH = 6.3. Deuterated solution samples were obtained by dialyzing protonated solutions in 33 mM phosphate D₂O buffer at pH (measured) = 5.9.

Single crystals of horse acid ferric hemoglobin have monoclinic crystal structure, two molecules per unit cell, and belong to the C₂ space group (Perutz, 1954). Since each molecule has an axis of dyad symmetry, the two molecules in the unit cell are magnetically equivalent. The spectra consist of electronic transitions from the iron atom in each of the four chains.

Spectra were obtained at 4.2K with a Varian X-band 4500 EPR spectrometer (Varian Associates, Palo Alto, Calif.). During cooling, the measured rate of temperature drop of the cavity was 1.2–1.6 K/min in the range 285–195 K, and a protein crystal would be frozen at this rate. No crystal was refrozen.¹ For single crystals of ferric hemoglobin fluoride and ferric myoglobin fluoride, Yonetani and Leigh (1971) found the temperature dependence of the line width to be remarkably small, and were able to show that the angular disorder was the same at 77K and 20 C. However, in the aquo complexes of ferric hemoglobin investigated here, the line widths at room temperature are too large (due to lifetime broadening) for resonances to be observed.

A TE₁₀₂ cavity and probe were built for use in a stainless steel Janis Dewar flask (Janis Research Co., Inc., Stoneham, Mass.). The crystal was mounted on a quartz rod that could rotate about its own axis. Rotation of the crystal holder and the magnet provided a method for obtaining all orientations of the crystal from one mounting except for a cone of ~30° centered on the crystal rotator axis. The microwave power at the sample was less than 0.25 mW at a frequency of 9.284 GHz. Power saturation studies show that at microwave powers higher than 0.25 mW, the trough line width increases nearly linearly with the square root of power. First derivative (of the absorption) spectra were obtained with 100 kHz field modulation. Modulation frequencies of 400 and 80 Hz show no change in trough line width from those obtained at 100 kHz.

Computer programs for the spectra simulation were written in FORTRAN for use on a CDC CYBER 172 computer (Control Data Corp., Minneapolis, Minn.). The *g*-tensors were determined from multiple orientation data where the six elements of each *g*-tensor were simultaneously determined by a least squares computer fit.

RESULTS

g-tensor information obtained from these orientation studies is listed in Table I. Note that there are small amounts of rhombic character in both the α - and β -chains.

The resonances, displayed as the first derivative of the absorption, show large variations in shape and width. At *g* = 6 the peak-to-trough width (LW_{p-t}) is about 30 G (Fig. 1, left), increases to 300–400 G in the region between *g* = 2 and 3 (Fig. 1, right); and then decreases to about 24 G at *g* = 2 (Fig. 2A, B). Furthermore, at *g* = 2, the single crystal resonance appears more like that from a polycrystalline sample,² and some of this resonance persists as the magnetic field is moved many degrees away from the heme normal (Fig. 2 B, C).

Line shape and width variations of these magnitudes have been suggested as arising from distribution in direction or magnitude of one or more spin Hamiltonian terms. For example,

¹EPR spectra from some crystals have been found to deteriorate progressively when the protein is cycled between room and cryogenic temperatures (Brill and Venable, 1964; Yonetani and Schleyer, 1967).

²Peaks (troughs) having the shape of absorption lines appear in the first derivative spectra of frozen solution and powder samples as the magnetic field strength enters (leaves) the region of EPR absorption.

TABLE I
 PRINCIPAL g VALUES AND ANGLES
 BETWEEN THE $g = 2$ DIRECTIONS

g-values				
α_1	1.978 ± 0.012	5.730 ± 0.009	6.016 ± 0.014	
α_2	1.970 ± 0.022	5.720 ± 0.008	6.012 ± 0.008	
β_1	1.970 ± 0.029	5.895 ± 0.013	5.924 ± 0.010	
β_2	1.981 ± 0.008	5.904 ± 0.010	5.927 ± 0.014	

Angles between the $g = 2$ directions*				
	α_1	α_2	β_1	β_2
α_1	0	55.1	59.9	13.4
α_2	(1.2)	0	13.4	59.7
β_1	(0.9)	(1.8)	0	61.1
β_2	(1.8)	(0.7)	(0.5)	0

*Each number in parenthesis is the difference between the angular separation of the $g = 2$ directions and the separation of the corresponding pair of heme normals in the X-ray-determined structure.

the broadening mechanism in acid ferric myoglobin has been explained in terms of a slight random misorientation of the molecular axes within the crystal, resulting in a spread in the principal directions of the g -tensors (Helcké et al., 1968; Eisenberger and Pershan, 1967; see also Mailer and Taylor, 1972). A distribution of g -values for any given magnetic field orientation is thus obtained. This same effect is generated by the mosaic model in which a nearly perfect crystal is composed of crystallites making very small angles with each other (Wenzel

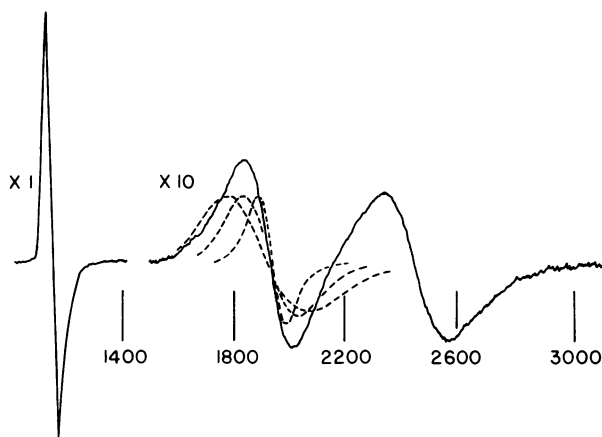


FIGURE 1 Experimental spectrum with four resonances, two coalesced in the $g = 6$ region (1,140 G, to the left) and two resolved in the $g = 3-2$ region ($\sim 3,300$ to $\sim 2,000$ G, center and right). The two resonances in the latter region differ greatly from one another in line width. The dashed curves show simulation of the 1,930 G resonance for $\eta_D = 1.7^\circ, 3.5^\circ,$ and 5.2° . In all cases the first derivative of the absorption is shown.

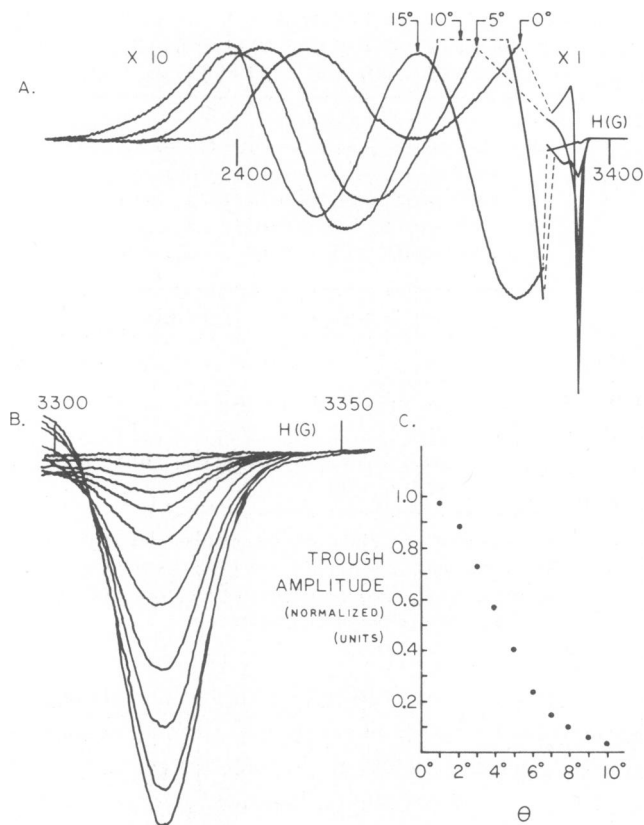


FIGURE 2 Experimental spectra for the rotation of the external field away from the heme normal (A) for two resonances in 5° increments and (B) for one resonance in 1° increments in the $g = 2$ region alone. (C) Plot of normalized trough amplitude versus rotation angle θ .

and Kim, 1965; Kirkby and Thorp, 1968; Shaltiel and Low, 1961). In addition to orientation disorder, spread in the crystal field splittings has been invoked to explain line broadening. For example, the model of Calvo and Bemski (1976), based upon intramolecular disorder, effectively accounts for the EPR line width variation in the heme plane of ferric myoglobin crystals, but does not apply to the behavior at $g = 2$ shown in Fig. 2 and requires a very large distribution in two of the spin Hamiltonian parameters to explain the line widths in the region between $g = 2$ and 6.

As with acid ferric myoglobin, the major source of broadening in single crystals of ferric hemoglobin is probably orientation disorder of the heme group. To use single crystal EPR spectra to obtain information about the interaction of a magnetic center with its environment from unresolved hyperfine interactions and other line width effects, it is necessary to incorporate the consequences of disorder in a quantitative way, and this is done below in a manner different from the earlier treatments of data from other protein crystals. Previously a single formula was used, which relates a disorder angle to the observed peak-to-trough line width by a factor that depends upon the orientation of the magnetic field. In the present treatment the effects of disorder are simulated and the results provide a more ac-

curate means of estimating the disorder angle. Furthermore the earlier method was applied to data from ferric myoglobin crystals, where, apparently (original spectra are not shown in the literature), approximately normally shaped single crystal resonances are observed in the $g = 2$ direction, a peak-to-trough line width can be measured, and no special analysis is required for this direction. From ferric hemoglobin crystals, the subject of the present paper, the EPR spectra exhibit essentially only a trough in the $g = 2$ region, a case not treated in the literature.

DISORDER ANALYSIS

We assume that there is a distribution only in the principal directions and not in the principal g -values.³ In the calculations that follow of the resulting EPR effects, the principal axes are fixed and the magnetic field direction is given an axially symmetric distribution function, a probability per unit solid angle to be called P_H . This is equivalent to having identical, axially symmetric disorder at each of the three g axes, with a single angle characterizing the degree of disorder. If the g -tensor is axial, the model used in the calculations still requires the disorder in g_z to be axially symmetric about its most probable direction, Z_0 , but is consistent with any disorder of g_x and g_y in the plane perpendicular to Z_0 .

The function P_H is assumed here to be Gaussian:

$$P_H^l = \exp [-(l\Delta\eta/\eta_D)^2] \quad (1)$$

where $\Delta\eta$ is the angle between adjacent solid angle centers. $l (= 0, 1, 2, \dots)$ is an index that increments $\Delta\eta$ away from the most probable orientation, that for which $P_H = P_H^0 = 1$. η_D is termed the disorder angle and represents that angle within which approximately 63% of the total orientations are to be found for disorder angles less than 20° .

The simulation of EPR spectra for disordered single crystals requires a method for the generation of the solid angles. It is impossible to lay down a grid of equal solid angles on a spherical surface for finite $\Delta\eta$. There will be inherent errors from any method chosen to approximate the solid angles. The simplest method is to define the center of the first solid angle as that orientation of \mathbf{H} that corresponds to $P_H^0 = 1$, as shown in Fig. 3. This area is a spherical cap of arc length from center to edge equal to $\Delta\eta/2$. Other solid angles are generated on annuli with boundaries $\Delta\eta/2 \rightarrow 3\Delta\eta/2, 3\Delta\eta/2 \rightarrow 5\Delta\eta/2$, etc. The centers of these rings are located at angles $l\Delta\eta$ ($l = 1, 2, 3, \dots$) from the $P_H^0 = 1$ direction. The number of solid angles on the l^{th} ring is given by $2\pi \sin l\Delta\eta/\Delta\eta$, and rounded off to an integer. In this manner, a grid of solid angles may be generated over the entire sphere. Although the constancy of the areas depends upon $\Delta\eta$, the standard error in the solid angles is in general less than 0.6%. The largest contributing sources to the error are those solid angles in the center, and in the first and second circles. Since the change of g from one solid angle to another is made small, no attempt to reduce the error was made.

To the orientation at the center of each solid angle corresponds a probability P_H^i , a g -value, and a transition probability P_{Tr}^i . The g -value determines a magnetic field strength

³This assumption simplifies the analysis and is supported by the data. There can be a distribution in principal g values as well. Although in solution the latter distribution makes a significant contribution to the component line width, in crystals (H_2O) the contribution is found to be negligible compared with dipolar broadening (Brill and Hampton, 1979).

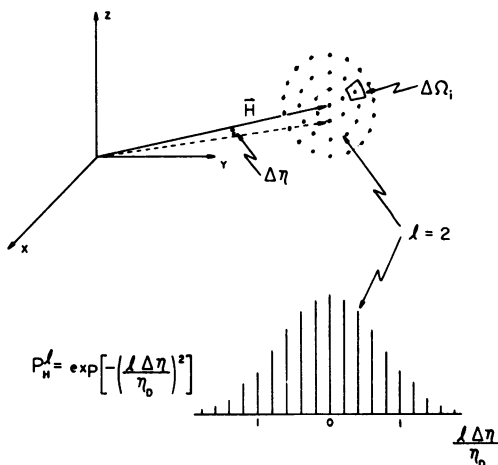


FIGURE 3

FIGURE 3 Generation of the solid angles on the unit sphere in increments of $\Delta\eta$. The probability distribution is cylindrical and Gaussian.

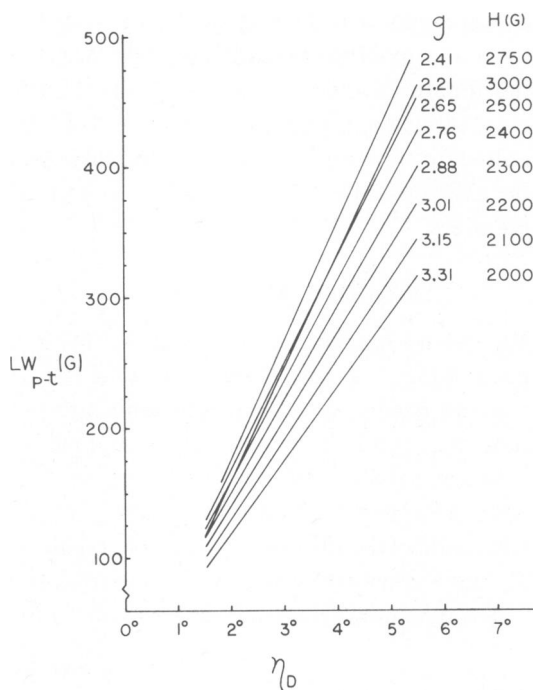


FIGURE 4

FIGURE 4 Peak to trough line width, LW_{p-t} , of simulated spectra versus disorder angle for various g values (resonant magnetic fields).

to which must be added and subtracted splittings due to hyperfine interactions in order to obtain the resonance fields, H' , arising from this orientation. Upon weighting these resonances by the product $P_H^i P_{Tr}^i$ and repeating this process for the entire grid of solid angles, one obtains a density distribution $D(H')$ [$D(H')\Delta H'$ is the number of resonances between H' and $H' + \Delta H'$] for the nominal (most probable) orientation.

In the heme protein cases treated here, the calculated spectral density, $G(H)$, in the region H to $H + \Delta H$, can be expressed as

$$G(H) = \sum_{H'} f(H - H', H') D(H') \Delta H' \quad (2)$$

where $f(H - H', H')$ is the component line shape function of unit area; i.e., the resonance envelope of any member of the sum for $D(H')\Delta H'$. This equation is valid for line shape functions whose line widths and shapes are constant or vary only with respect to H' . For orientation-dependent functions, Eq. 2 cannot be used for the simulation of spectra, since each member in the sum for $D(H')\Delta H'$ may now have a different envelope width and/or shape.

By comparing simulated spectra with those of experiment, two independent methods for determining disorder angles and shapes have been developed. One method makes use of

the fact that the peak-to-trough line width, LW_{p-t} , is large in the $g = 2-3$ region, as shown in Fig. 1, right. The simulated spectral density, $G(H)$, of Eq. 2, written in integral form, is

$$G(H) = \int f(H - H') D(H') dH' \quad (3)$$

As will be shown below, $G(H)$ in this region of g is essentially independent of the component line shape function, $f(H - H')$, so that Eq. 2 is applicable. The component line shape function is written here as an absorption, not some derivative. The derivative $dG(H)/dH$ is to be computed and its peak to trough line width compared with that of the experiment. From the angular dependence of the pyrrole nitrogen hyperfine coupling constants (Scholes, 1970) and estimates of that of the proximal imidazole nitrogen, the line width of the total envelope function $f(H - H')$ is calculated to be less than 20 G. The spread in $G(H)$ is due to the large spread in the density distribution $D(H')$. Thus $f(H - H')$ is small compared to $D(H')$ and may be replaced by a δ function and integrated:

$$G(H) \propto \int \delta(H - H') D(H') dH' = D(H) \quad (4)$$

for absorption. For first derivative spectra, $dG(H)/dH \propto dD(H)/dH$. A spectrum in the $g = 2-3$ region is proportional to the density distribution and would be sensitive to the probability distribution, P_H .

A plot of simulated spectra LW_{p-t} versus disorder angle at various resonant fields for g -values in the $g = 2-3$ range is given in Fig. 4. The spectra were simulated for component line widths of 5, 10, and 20 G and no variation in the measured points was obtained. This clearly demonstrates the independence of $G(H)$ on $f(H - H')$ in this region. The disorder angle of a crystal may be determined from a transition in this range of g values from Fig. 4 once LW_{p-t} and the approximate resonance magnetic field have been measured. Information about the shape of the disorder function is obtained by comparing simulated and experimental spectra directly.

An independent method for determining disorder angles and shapes involves the analysis of spectra at a g -extremum separated in magnetic field from the other two g -values by an amount larger than the resonance line widths. At X-band, the $g = 2$ resonances in the aquo complex of ferric hemoglobin are about 2,000 G away from the $g = 6$ resonances. Because of disorder the $g = 2$ resonance persists as the magnetic field is moved many degrees away from the heme normal, as shown in Fig. 2A for 5° rotation increments. Two resonances are present in the spectra and both move downfield upon rotation of \mathbf{H} . Fig. 2B shows 1° rotations of \mathbf{H} in the $g = 2$ region alone. The fall off in the trough amplitude, when normalized and plotted against rotation angle, as in Fig. 2C, appears to be Gaussian and to contain disorder information.

Spectra were simulated in the $g = 2$ direction by means of the known nitrogen coupling constants obtained from ENDOR data with the magnetic field parallel to the heme normal in frozen solutions of human hemoglobin (Feher et al., 1973). In detail, the imidazole nitrogen splitting was held constant at 4.10 G while the pyrrole nitrogen splittings (2.76 G at $g = 2$) varied with orientation as given by Scholes (1970).⁴ The component line is defined in this

⁴The behavior of the imidazole nitrogen splitting in the $g = 2$ direction is like that of the pyrrole nitrogen splitting in the $g = 6$ direction; it changes slowly as the magnetic field moves away from the heme normal.

method as the single resonance in the absence of known nitrogen splittings, of width determined by such factors as dipolar interactions, distribution in principal g values, and lifetime broadening. For Gaussian disorder, simulated spectra for a series of rotations θ of the magnetic field away from the $g = 2$ direction exhibit the characteristics of those of experiment, Fig. 5 A. If the normalized amplitude has a Gaussian dependence upon rotation angle,

$$A_i/A_{\max} = \exp [-(\theta_i/\eta_D^M)^2] \quad (5)$$

and transforming the Gaussian function to a straight line

$$\{-\ln(A_i/A_{\max})\}^{1/2} = \theta_i/\eta_D^M \quad (6)$$

one finds that the fall off in the $g = 2$ resonance of the simulated spectra does indeed show the Gaussian nature of the disorder as shown in Fig. 5 B. The "measured" disorder angle, η_D^M , characterizes the fall off in trough amplitude and is the inverse slope in Eq. 6. For various values of component line widths and choices of the magnetic field at which the amplitude is measured, the simulated spectra show $\eta_D \leq \eta_D^M \leq 1.1 \eta_D$. Lorentzian disorder can be treated analogously, and the falloff in trough amplitude is then found to be Lorentzian with $\eta_D \leq \eta_D^M \leq 1.2 \eta_D$. The type of disorder present can be diagnosed from the behavior for $\theta > \eta_D^M$. For example, in the case of triangular disorder, the amplitude measured at $g = 2$ rapidly vanishes beyond $\theta = \eta_D^M$.

RESULTS OF ANALYSIS AND DISCUSSION

Application of the two preceding methods for heme disorder analysis in single crystals of horse ferric hemoglobin shows that the shape of the distribution is Gaussian, more so for the transitions in the α -chain than in the β -chain, where the distribution function is slightly broader in the wings than Gaussian. The latter is apparent in the $g = 2-3$ region, where the wings of the β -chain first derivative resonances are more intense than those of the α -chains. This observation suggests that, in addition to the intermolecular disordering of the molecules within the crystal, there is an intramolecular disordering. (Disorder of the terminal residues and the side chains of penultimate tyrosines is apparent in the structure of horse ferric hemoglobin at 2.0 Å resolution; Ladner et al., 1977). The magnitudes of the disorder angles for α - and β -chains in the crystals studied varied from 3.6° to 4.6°. Since both methods give this range of disorder and apply to very different orientations of the polarizing magnetic field, it follows that the disorder is constant over the sphere. The latter result is consistent with the model of disorder which has been employed.

The magnitudes of the disorder angles can be compared with the angular spread from X-ray data.⁵ G. Fermi, in an appendix to the paper by Ladner et al., 1977, estimates the root mean square (rms) error in position of the atoms of the heme plane to be as small as 0.14 Å, although the overall positional error is 0.25 Å in horse ferric hemoglobin crystals. Taking the average heme radius to be about 4 Å, one finds rms angular errors in the normal to the heme plane to be 2.0° for the 0.14 Å value and 3.6° for 0.25 Å. For comparison with

⁵We thank Dr. Elizabeth G. Heidner for suggesting the mode employed here of calculating the angular error from X-ray data.

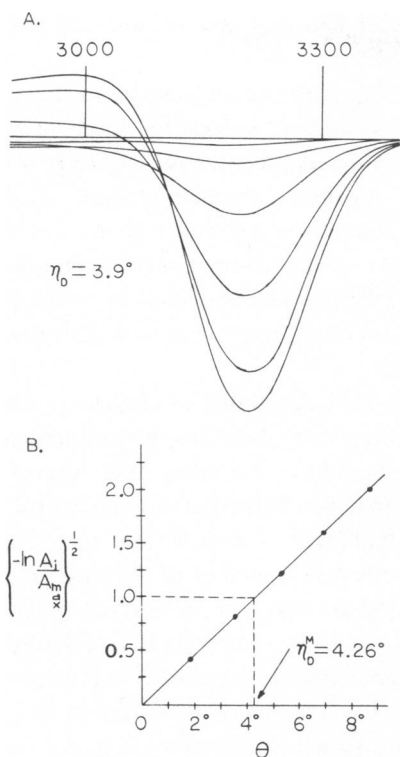


FIGURE 5

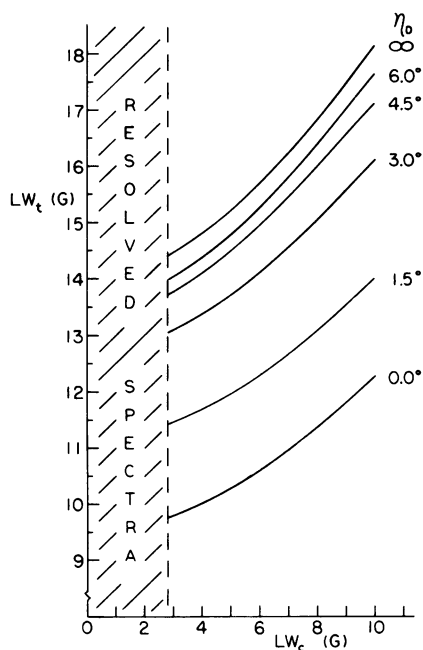


FIGURE 6

FIGURE 5 (A) Simulated spectra in the $g = 2$ region for rotation of the external field away from the heme normal in $\sim 1.8^\circ$ increments for a Gaussian disorder with disorder angle $\eta_D = 3.9^\circ$. (B) Plot of the square root of minus the natural logarithm of the normalized amplitude measured at maximum trough amplitude in A versus rotation angle showing the measured disorder angle η_D^M .

FIGURE 6 Plot of the full width at half maximum, LW_t , of the first derivative trough at $g = 2$ versus component line width, LW_c , for various disorder angles. Values of LW_t and η_D for frozen solutions and single crystals correspond to specific component line widths.

TABLE II

DISORDER ANGLES, TROUGH WIDTHS OF THE $g = 2$ RESONANCE, AND COMPONENT LINE WIDTHS FOR THE FERRIC ION IN HEMOGLOBIN CHAINS UNDER VARIOUS EXPERIMENTAL CONDITIONS

Sample	Mother liquor	Chain	η_D	LW_t	LW_c
Single crystals	H_2O	α	$3.6^\circ-4.6^\circ$	G	G
		β	$3.8^\circ-4.3^\circ$	14.0-14.5	4.0-5.5
	D_2O	α	$3.7^\circ-4.2^\circ$	14.1-14.4	4.3-5.6
		β	$3.7^\circ-4.2^\circ$	14.2-14.4	4.6-5.6
Frozen solutions	H_2O	All	∞	15.7-16.1	6.1-6.8
		four	∞	15.0-15.3	4.5-5.2
	D_2O	All	∞	15.7-16.1	6.1-6.8
		four	∞	15.0-15.3	4.5-5.2

η_D , these angles must be multiplied by $\sqrt{2}$. Between the resulting values, 2.8° and 5.1° , lies the range of disorder angles reported here, 3.6° – 4.6° .

The α - and β -chain disorder angles and the $g = 2$ experimental and simulated spectra may be used to obtain information about the interaction of the iron with its environment through the component line as defined under method two. One characterization of the $g = 2$ resonance is the full width at half maximum, LW_i , of the first derivative trough. A plot of LW_i for simulated spectra versus peak-to-trough component line width, LW_c , for various disorder angles is shown in Fig. 6. By measuring LW_i of an experimental spectrum, the component line width may be obtained from Fig. 6 once the disorder angle has been determined. Typical values for LW_i are in the range from 14.0 to 14.6 G, increasing with disorder angle. Table II shows the resulting component line widths.

Changes in the environment of an iron atom should be detectable by changes in the component line width. Several deuterated crystals were prepared and varying degrees of disorder were found, increasing with preparatory soak time. One infers that loss of inter- and/or intramolecular integrity proceeds as exchangeable hydrogen is replaced by deuterium. The experimental results for the crystal that had the least disorder are $\eta_D \sim 3.7^\circ$ – 4.2° and $LW_i \sim 14.1$ – 14.4 G, and correspond to component line widths of 4.3–5.6 G. These parameters for a crystal that was allowed to soak for 1 wk are $\eta_D \sim 6.0^\circ$ – 7.5° and $LW_i \sim 16.1$ G, corresponding to component line widths of 6.7–7.6 G. The facts that the component line width for the least disordered crystal is in the same range of values as that for protonated crystals and that it increases dramatically with soak time suggest additional sources of broadening in the deuterated crystals. In particular, structural variation characterized by a distribution in the crystal field parameters of the spin Hamiltonian would yield a distribution in principal g values and, consequently, lead to line broadening.

The method was also applied to frozen solutions where $\eta_D = \infty$. All four hemes now contribute to the $g = 2$ resonance. Experimentally it is found that in single crystals the trough maxima for α - and β -chains differ by approximately 1.6 G or 0.001 in g . This difference contributes ~ 0.15 G to LW_i in frozen solution spectra. The $\eta_D = \infty$ curve in Fig. 6 does not incorporate this effect, because the spectra leading to these curves were simulated for an isolated heme. Measured values of LW_i for protonated and deuterated frozen solutions are 15.7–16.1 and 15.0–15.3 G, respectively. The component line width determined from Fig. 6 for the protonated solutions is 6.1–6.8 G, greater than those for the single crystals. As will be discussed in the following paper (Brill and Hampton, 1979), dipolar broadening quantitatively accounts for the observed line widths in single crystals. Since the only difference in dipolar interaction from single crystals to frozen solutions is the reduced intermolecular ferric dipole-ferric dipole contribution, the fact that the frozen solution shows a greater component line width indicates the existence of a broadening mechanism not presently included in the analysis given above. Other experiments are needed to determine the origin of this extra broadening.

This research was supported by grants from the National Heart, Lung and Blood Institute, the U.S. Public Health Service (HL-13989), and the National Science Foundation (PCM 76-83841).

Received for publication 25 March 1978.

REFERENCES

- BRILL, A. S., and D. A. HAMPTON. 1979. Quantitative evaluation of contributions to electron paramagnetic resonance linewidths in ferric hemoglobin single crystals. *Biophys. J.* **25**:313-322.
- BRILL, A. S., and J. H. VENABLE, JR. 1964. Electron paramagnetic resonance in single crystals of cupric insulin. *Nature (Lond.)* **203**:752-754.
- BRILL, A. S., and R. J. P. WILLIAMS. 1961. The absorption spectra, magnetic moments, and the binding of iron in some haemoproteins. *Biochem. J.* **78**:246-253.
- BRILL, A. S., C.-I. SHYR, and T. C. WALKER. 1975. Power saturation of electron paramagnetic resonances from high-spin ferric haemoproteins at 4.2 K. *Mol. Phys.* **29**:437-454.
- CALVO, R., and G. BEMSKI. 1976. On the electron spin resonance linewidths of metmyoglobin. *J. Chem. Phys.* **64**:2264-2265.
- EISENBERGER, P., and P. S. PERSHAN. 1967. Magnetic resonance studies of met-myoglobin and myoglobin azide. *J. Chem. Phys.* **47**:3327-3333.
- FEHER, G., R. A. ISAACSON, C. P. SHOLES, and R. NAGEL. 1973. Electron nuclear double resonance (ENDOR) investigation on myoglobin and hemoglobin. *Ann. N. Y. Acad. Sci.* **222**:86-101.
- HELCKÉ, G. A., D. J. E. INGRAM, and E. F. SLADE. 1968. Electron resonance studies of hemoglobin derivatives. III. Line-width and g-value measurements of acid-metmyoglobin and of metmyoglobin azide derivatives. *Proc. R. Soc. Lond. B. Biol. Sci.* **169**:275-288.
- KIRKBY, C. J., and J. S. THORP. 1968. Inhomogeneous electron paramagnetic resonance line broadening in ruby. *J. Phys. C. Solid State Phys.* **1**:913-918.
- LADNER, R. C., E. J. HEIDNER, and M. F. PERUTZ. 1977. The structure of horse methaemoglobin at 2.0 Å resolution. *J. Mol. Biol.* **114**:385-414.
- MAILER, C., and C. P. S. TAYLOR. 1972. Electron paramagnetic resonance study of single crystals of horse heart ferricytochrome c at 4.2° K. *Can. J. Biochem.* **50**:1048-1055.
- PERUTZ, M. F. 1954. The structure of haemoglobin. III. Direct determination of the molecular transform. *Proc. R. Math. Phys. Sci. Soc.* **A225**:264-286.
- PERUTZ, M. F. 1968. Preparation of haemoglobin crystals. *J. Cryst. Growth.* **2**:54-56.
- SHOLES, C. P. 1970. EPR studies on heme oriented in an organic crystalline environment. *J. Chem. Phys.* **52**:4890-4895.
- SHALTIEL, D., and W. LOW. 1961. Anisotropic broadening of linewidth in the paramagnetic resonance spectra of magnetically dilute crystals. *Phys. Rev.* **124**:1062-1067.
- WENZEL, R. F., and Y. W. KIM. 1965. Linewidth of the electron paramagnetic resonance of $(\text{Al}_2\text{O}_3)_{1-x}(\text{Cr}_2\text{O}_3)_x$. *Phys. Rev.* **A140**:1592-1598.
- YONETANI, T., and J. S. LEIGH, JR. 1971. Electromagnetic properties of hemoproteins. IV. Single crystal electron paramagnetic resonance spectroscopy of hemoproteins at ambient temperature. *J. Biol. Chem.* **246**:4174-4177.
- YONETANI, T., and H. SCHYLEYER. 1967. Electromagnetic properties of hemoproteins. I. Electron paramagnetic resonance absorptions of single crystals of ferrimyoglobin and cytochrome c peroxidase. *J. Biol. Chem.* **242**:3919-3925.